

A Hamiltonian electromagnetic gyrofluid model

F. L. Waelbroeck, R. D. Hazeltine, and P. J. Morrison

Institute for Fusion Studies, University of Texas, Austin, Texas 78712, USA

(Received 19 August 2008; accepted 2 February 2009; published online 20 March 2009)

An isothermal truncation of the electromagnetic gyrofluid model of Snyder and Hammett [Phys. Plasmas **8**, 3199 (2001)] is shown to be Hamiltonian. The corresponding noncanonical Lie–Poisson bracket and its Casimir invariants are presented. The invariants are used to obtain a set of coupled Grad–Shafranov equations describing equilibria and propagating coherent structures.

© 2009 American Institute of Physics. [DOI: [10.1063/1.3087972](https://doi.org/10.1063/1.3087972)]

I. INTRODUCTION

Fluid models of plasma dynamics have proven fruitful in bringing to light new nonlinear phenomena such as solitary kinetic Alfvén waves,¹ streamers,² generation of geodesic acoustic modes,^{3,4} fast reconnection mediated by whistler⁵ and kinetic Alfvén waves,^{6,7} mechanisms for the onset of fast reconnection,⁸ partial reconnection,⁹ and phase mixing in collisionless reconnection.¹⁰ In some cases fluid models have been used to explain the results of kinetic simulations of turbulent transport.¹¹ A subset of the fluid models, referred to as “cold ion” models because they assume that $T_i \ll T_e$, has been shown to possess a noncanonical Hamiltonian formulation.^{12–14} Attempts to find such formulations for models with $T_i \sim T_e$, however, have met with mixed success. The difficulty resides primarily in the nonlocality of the ion dynamics caused by the excursions of the ions in their Larmor gyration.

A particularly important class of fluid models is the flute-reduced models that exploit the ordering $k_{\parallel} \ll k_{\perp}$, where k_{\parallel} is the component of the wavevector \mathbf{k} in the direction of the background magnetic field \mathbf{B}_0 and k_{\perp} is the component perpendicular to \mathbf{B}_0 . Within the class of flute-reduced hot-ion models, it is convenient to distinguish those that approximate the nonlocal terms through a Taylor-series expansion based on a long-wavelength approximation, $\rho_i k_{\perp} \ll 1$,^{15,16} and those that attempt to account for the full range of perpendicular wavevectors by using nonlocal averaging operators.^{17–20} We will refer to the first as finite Larmor radius (FLR) models and the second as gyrofluid models.

Electrostatic fluid models using both the FLR (Ref. 21) and gyrofluid^{17,18} approaches have been available for many years. Both approaches have played a key role in advancing the understanding of turbulent transport. A few years ago, Krommes and Koleshnikov²² presented a Hamiltonian formulation for a simple gyrofluid model due to Rogers *et al.*,¹¹ evolving the density and ion temperature. They showed how to use the Hamiltonian property of the system to calculate the generation of long-wavelength structures, such as zonal flows, by short-wavelength turbulence. Shortly thereafter Waelbroeck *et al.*²³ presented a Hamiltonian formulation for a FLR model of ion-temperature gradient driven turbulence proposed by Kim *et al.*²⁴ They pointed out the role of the Hamiltonian property in the existence of ideal coherent structures (ideal coherent structures are characterized by a

balance between dispersion and nonlinear steepening, in contrast to dissipative coherent structures where steepening is balanced by dissipative transport). They also provided an example of how the lack of Hamiltonian structure could result in the equilibrium equation being insoluble. The role of the Hamiltonian formulation in the existence of ideal coherent structures is reviewed briefly in Sec. V of the present paper.

Electromagnetic fluid models, like their electrostatic counterparts, have played an important role in advancing the understanding of plasma dynamics. In particular, electromagnetic fluid models are the primary means of interpreting the observations of nonlinear structures in the magnetopause²⁵ and in the edge of laboratory experiments.²⁶ Thus, it is not surprising that efforts to construct electromagnetic Hamiltonian models for hot-ion plasma dynamics preceded similar efforts for electrostatic models by over a decade. Hazeltine *et al.* constructed the first such Hamiltonian FLR model by using a mapping technique.²⁷ Unfortunately, the dispersion relation for the linearized version of their model, although correct in the long-wavelength limit, has undesirable features at short wavelengths that have inhibited its widespread adoption. More recently, Schep and co-workers proposed a gyrofluid model [Schep–Pegoraro–Kushinov (SPK)] along with a generating noncanonical Poisson bracket.^{28,29} The SPK bracket, however, fails to satisfy the Jacobi identity (we give a counterexample in Appendix A) and is thus disqualified as a Poisson bracket. Lastly, we note that Strinzi *et al.* also used Lagrangian methods to construct gyrofluid models satisfying desired conservation properties.³⁰

In the present paper, we describe a simple electromagnetic gyrofluid model that possesses a noncanonical Hamiltonian formulation. Our model is a severe truncation of the much more complete model proposed by Snyder and Hammett that advances six moments for the ions and two moments for the electron dynamics.¹⁹ These authors showed that their model reproduces exactly the kinetic dispersion relation. They did not, however, address the question of its Hamiltonian nature. Grasso *et al.* by contrast used a minimal Hamiltonian electromagnetic gyrofluid model to investigate hot-ion effects in magnetic reconnection.³¹ Their model assumes that the density of ion guiding centers is unperturbed and it evolves only the magnetic flux and the particle density. The orbit-averaging effects are described by a Padé approxi-

mation of the response of the particle density to the electrostatic potential. Loureiro and Hammett also investigated magnetic reconnection with a model similar to that of Grasso *et al.* except that they used Bessel functions to achieve a more accurate description of the orbit-averaging effects.²⁰

The model we investigate here extends the models of Grasso *et al.*³¹ and Loureiro and Hammett²⁰ by additionally evolving the ion guiding center density. This enables our model to describe drift waves and the effects of diamagnetic flows associated with inhomogeneous plasma. With the inclusion of transport terms, our model is also able to describe relatively slow processes, such as tearing modes, where the density and velocity profiles may evolve under the effect of collisional transport processes.

II. FORMULATION

We are interested in a model that describes the interaction of kinetic Alfvén waves with drift waves. In order to avoid complications associated with the sound wave, ion parallel motion, and ion Landau damping, we assume that $k_{\parallel}v_{ti} \ll \omega_*$, where v_{ti} is the ion thermal velocity and ω_* is the drift frequency. We leave β_e unrestricted, by contrast, in order to describe both the “inertial” ($\beta_e \ll m_e/m_i$) and the “kinetic” ($\beta_e \gg m_e/m_i$) regimes of the Alfvén wave³² (β_e is the ratio of the electron kinetic pressure to the magnetic pressures). For $\beta_e \sim m_e/m_i(v_{te} \sim v_A)$, however, our equations must be augmented with a model for electron Landau damping. We consider the evolution of the density of the ion guiding centers n_i , the electron density n_e , and the magnetic flux $\psi = -A_z$ where \mathbf{A} is the vector potential. The quasineutrality condition determines the electrostatic potential ϕ . We normalize these quantities according to

$$(n_i, n_e, \psi, \phi) = \frac{L_n}{\rho_s} \left(\frac{\hat{n}_i}{n_0}, \frac{\hat{n}_e}{n_0}, -\frac{\hat{A}_z}{\rho_s B_0}, \frac{e\hat{\phi}}{T_{e0}} \right),$$

where the carets denote the dimensional variables. Here n_0 is the background density, $\rho_s = c_s/\omega_{ci}$ where $c_s = (T_e/m_i)^{1/2}$ is the sound speed, $\omega_{ci} = eB_0/m_i$ is the ion cyclotron frequency, and $L_n = n_0/|\nabla n|$ is the density scale length. We also normalize the independent variables according to

$$(t, k_{\parallel}, k_{\perp}) = (\hat{t}c_s/L_n, \hat{k}_{\parallel}L_n, \hat{k}_{\perp}\rho_s).$$

Normalizing the perpendicular lengths to ρ_s has the advantage of making the $\tau = T_i/T_e \rightarrow 0$ limit transparent.

The evolution equations are obtained from the equations of Ref. 19 by assuming constant temperatures for both the ions and electrons and discarding all but the lowest-order moment for the ions and the lowest two parallel moments for the electrons. They are

$$\frac{\partial n_i}{\partial t} + [\Phi, n_i] = 0, \quad (1)$$

$$\frac{\partial n_e}{\partial t} + [\phi, n_e] - c_A^2 \nabla_{\parallel} J = 0, \quad (2)$$

$$\frac{\partial}{\partial t}(\psi - d_e^2 J) - d_e^2[\phi, J] + \nabla_{\parallel}(n_e - \phi) = 0, \quad (3)$$

where $\nabla_{\parallel} \xi = \partial_z \xi + [\psi, \xi]$ for any field ξ , $J = J_z = \nabla^2 \psi$ is the axial current, $d_e^2 = 2m_e/(m_i \beta_e)$ is the square of the electron skin depth normalized to ρ_s , $c_A = (2/\beta_e)^{1/2}$ is the Alfvén speed normalized to the sound speed, and

$$\Phi = \Gamma_0^{1/2} \phi$$

is the gyroaveraged electrostatic potential. Here $\Gamma_0^{1/2}$ is an operator introduced by Dorland and Hammett¹⁸ and defined by

$$\Gamma_0^{1/2} \xi = \exp\left(\frac{1}{2} \tau \nabla_{\perp}^2\right) I_0^{1/2}(-\tau \nabla_{\perp}^2) \xi, \quad (4)$$

where I_0 is the modified Bessel function of the first kind and $\tau = T_i/T_e$. The definition in Eq. (4) should be interpreted in terms of its series expansion,

$$\Gamma_0^{1/2} \xi = 1 + \sum_{n=1}^{\infty} a_n (\tau \nabla_{\perp}^2)^n = 1 + (\tau/2) \nabla^2 + \dots,$$

where the a_n are real numbers. The system is completed by the quasineutrality equation,

$$n_e = \Gamma_0^{1/2} n_i + (\Gamma_0 - 1) \phi / \tau, \quad (5)$$

where $\Gamma_0 = (\Gamma_0^{1/2})^2$. The SPK model,²⁸ by contrast, can be obtained from the standard FLR model by replacing the perpendicular gradients by $[(\Gamma_0 - 1)/\tau]^{1/2}$. This procedure gives the correct result in the limit of long and short perpendicular wavelengths as well as (by construction) in the $\tau \rightarrow 0$ limit, but it is clearly less physically compelling than that of Ref. 19.

The above equations conserve the following energy:

$$H = \frac{1}{2} \langle c_A^2 (|\nabla \psi|^2 + d_e^2 J^2) + n_e^2 + \phi(1 - \Gamma_0) \phi / \tau \rangle, \quad (6)$$

where the angular brackets denote the integral over the volume of interest, $\langle g(x, y, z, t) \rangle = \int \int \int g(x, y, z, t) dx dy dz$, and the boundary conditions have been assumed to be such that the surface integrals vanish. Using the quasineutrality equation, the conserved energy may be written in more perspicuous form as

$$H = \frac{1}{2} \langle c_A^2 (|\nabla \psi|^2 + d_e^2 J^2) + \Phi n_i - \phi n_e \rangle.$$

In this form of the energy the successive terms represent, respectively, the magnetic energy, the kinetic energy in the electron parallel motion, the electron thermal energy, and the electrostatic energy of the ions and electrons. It is easy to show that the ion thermal energy is conserved separately: including it in the Hamiltonian lengthens the algebra unnecessarily.

For latter use we record here some properties of the operators $\Gamma_0^{1/2}$ and $\Gamma_0 - 1$. First, these operators and their inverses commute with each other, like any operator that is a sum of derivatives with constant coefficients. The operators are also formally self-adjoint; that is, if one integrates by parts term by term and neglects surface terms,

$$\langle f\Gamma_0^{1/2}g \rangle = \langle g(\Gamma_0^{1/2})^\dagger f \rangle = \langle g\Gamma_0^{1/2}f \rangle.$$

Finally, we have $\Gamma_0^{1/2}(\xi - cx) = \Gamma_0^{1/2}\xi - cx$, $\Gamma_0(\xi - cx) = \Gamma_0\xi - cx$, and $(\Gamma_0 - 1)(\xi - cx) = (\Gamma_0 - 1)\xi$, where c is any constant. These identities are useful when seeking traveling-wave solutions, and similar identities hold with x replaced by y .

III. HAMILTONIAN FORMULATION

A. Poisson bracket

We adopt n_i , n_e , and $\Psi = \psi - d_e^2 J$ as our dynamical variables. In terms of these variables the potential ϕ is given by the quasineutrality condition

$$\phi = \tau(\Gamma_0 - 1)^{-1}(n_e - \Gamma_0^{1/2}n_i), \quad (7)$$

and the Hamiltonian takes the form

$$H[n_i, n_e, \Psi] = \frac{1}{2}\langle c_A^2 \nabla \Psi \cdot (1 - d_e^2 \nabla^2)^{-1} \nabla \Psi + n_e^2 + \tau(n_e - \Gamma_0^{1/2}n_i)(1 - \Gamma_0)^{-1}(n_e - \Gamma_0^{1/2}n_i) \rangle. \quad (8)$$

Its variations are $H_{n_i} = \Phi$, $H_{n_e} = n_e - \phi$, and $H_\Psi = -2J/\beta_e$, where H_{ξ_j} is a shorthand notation for the functional derivative of $H[\xi_1, \xi_2, \xi_3]$ with respect to the fields $\xi_1 = n_i$, $\xi_2 = n_e$, $\xi_3 = \Psi$:

$$H_{\xi_j} := \frac{\delta H}{\delta \xi_j}, \quad j = 1, 2, 3.$$

We may write the equations of motion in terms of the variations of H as follows:

$$\frac{\partial n_i}{\partial t} = [n_i, H_{n_i}], \quad (9)$$

$$\frac{\partial n_e}{\partial t} = -\partial_z H_\Psi - [\Psi, H_\Psi] - [n_e, H_{n_e}], \quad (10)$$

$$\frac{\partial \Psi}{\partial t} = -\partial_z H_{n_e} - [\Psi, H_{n_e}] - \rho_e^2 [n_e, H_\Psi], \quad (11)$$

where $\rho_e^2 = \frac{1}{2}\beta_e d_e^2 = m_e/m_i$ is the electron gyroradius normalized to ρ_s . The corresponding Poisson bracket is

$$\{F, G\} = \{F, G\}_{\parallel} + \{F, G\}_{\perp}, \quad (12)$$

where

$$\{F, G\}_{\parallel} = \langle G_{n_e} \partial_z F_\Psi - F_{n_e} \partial_z G_\Psi \rangle \quad (13)$$

and

$$\begin{aligned} \{F, G\}_{\perp} = & \langle -n_i [F_{n_i}, G_{n_i}] + n_e ([F_{n_e}, G_{n_e}] + \rho_e^2 [F_\Psi, G_\Psi]) \\ & + \Psi ([F_\Psi, G_{n_e}] + [F_{n_e}, G_\Psi]) \rangle. \end{aligned} \quad (14)$$

This Poisson bracket can be shown directly to satisfy the Jacobi identity,

$$\mathcal{J} := \{F, \{G, H\}\} + \{G, \{H, F\}\} + \{H, \{F, G\}\} = 0 \quad (15)$$

for all functionals F , G , H by using the techniques developed in Ref. 33. In Sec. III C, however, we show this by simpler means.

B. Invariants

Casimir functionals are invariants of the motion that owe their existence to properties of the Poisson bracket.^{13,34} They are most useful in the presence of an ignorable coordinate because they can be used to construct variational principles for studying the equilibrium and stability of a system. In this section we assume $\partial_z = 0$: the generalization to the case of helical symmetry is straightforward and is described in Ref. 13.

We obtain the Casimir functional $C[n_i, n_e, \Psi]$ by expressing the condition that $\{\xi_j, C\} = 0$ for $\xi_j = n_i$, n_e , and Ψ . This results in the following system of equations:

$$[n_i, C_{n_i}] = 0, \quad (16)$$

$$[n_e, C_{n_e}] + [\Psi, C_\Psi] = 0, \quad (17)$$

$$\rho_e^2 [n_e, C_\Psi] + [\Psi, C_{n_e}] = 0. \quad (18)$$

The first equation is easily integrated,

$$C[n_i, n_e, \Psi] = \langle f(n_i) \rangle + G[n_e, \Psi], \quad (19)$$

where $G[n_e, \Psi]$ is a functional. The second equation, Eq. (17), imposes that $G[n_e, \Psi] = \langle g(n_e, \Psi) \rangle$ where g is an arbitrary function. The last equation, Eq. (18), becomes

$$\rho_e^2 g_{\Psi\Psi} - g_{n_e n_e} = 0.$$

Integrating this using the method of characteristics follows $G = G_{\pm}[n_e, \Psi]$ where

$$G_{\pm}[n_e, \Psi] = \langle g_{\pm}(\Psi \pm \rho_e n_e) \rangle, \quad (20)$$

and the g_{\pm} are an additional two arbitrary functions. The general form of the Casimir functional is thus

$$C[n_e, n_i, \Psi] = \langle f(n_i) \rangle + g_+(\Psi + \rho_e n_e) + g_-(\Psi - \rho_e n_e). \quad (21)$$

Note that in the limit $\rho_e \rightarrow 0$, the two Casimirs G_{\pm} become indistinguishable. In this limit a replacement Casimir is obtained from the first-order term in the Taylor expansion of G_{\pm} with respect to ρ_e . That is, the two Casimirs G_{\pm} are replaced by $\langle g(\psi) \rangle$ and $\langle n_e h(\psi) \rangle$ where $g = g_+ + g_-$ and $h = g'_+ - g'_-$.

In addition to Casimir invariants there are invariants, such as linear and angular momenta, that are not built into the Poisson bracket but depend on the choice of Hamiltonian. The following is an example of such for the system of Eqs. (1)–(3):

$$P_y[n_i, n_e] = \langle x(n_e - n_i) \rangle. \quad (22)$$

If one identifies $n_e - n_i$ with the vorticity, then this quantity is proportional to the y component of the total linear momentum. Its invariance follows upon time differentiating, inserting Eqs. (1)–(3), and making use of the properties of Γ_0 discussed at the end of Sec. II. Replacing x by y gives the x component of the linear momentum, and angular momentum is obtained similarly. In Sec. V we obtain a variational principle for equilibria; if P_y is added to this, one obtains equilibria in a frame moving uniformly in the y direction.

C. Normal fields and Jacobi

The form of the Casimirs suggests the introduction of a new set of variables, which we call “normal fields”: n_i and $\Psi_{\pm} = \Psi \pm \rho_e n_e$. In terms of these normal fields, the equations of motion take the form

$$\frac{\partial n_i}{\partial t} + [\Phi, n_i] = 0, \quad (23)$$

$$\frac{\partial \Psi_{\pm}}{\partial t} + [\phi_{\pm}, \Psi_{\pm}] = 0, \quad (24)$$

where

$$\phi_{\pm} = \phi \pm \psi / \rho_e$$

are stream-functions that describe flows that convect the fields n_i , Ψ_{\pm} . The latter are thus Lagrangian conserved quantities. Grasso *et al.*¹⁰ showed that the mixing of such Lagrangian quantities by the convecting flows is an important ingredient in rapid collisionless reconnection.

The Poisson bracket of Eq. (12) can be written in terms of the normal fields by making use of the transformation $n_i = n_i$, $\Psi = (\Psi_+ + \Psi_-)/2$, and $n_e = (\Psi_+ - \Psi_-)/2\rho_e$, which gives for the functional derivatives: $F_{n_i} = \bar{F}_{n_i}$, $F_{n_e} = \rho_e(\bar{F}_{\Psi_-} - \bar{F}_{\Psi_+})$, and $F_{\Psi} = \bar{F}_{\Psi_-} + \bar{F}_{\Psi_+}$. Dropping the overbars and inserting these derivatives into the brackets of Eqs. (13) and (14) gives

$$\{F, G\}_{\parallel} = 2\rho_e \langle G_{\Psi_-} \partial_z F_{\Psi_-} - G_{\Psi_+} \partial_z F_{\Psi_+} \rangle, \quad (25)$$

and

$$\begin{aligned} \{F, G\}_{\perp} = & -\langle n_i [F_{n_i}, G_{n_i}] \rangle + 2\rho_e \langle \Psi_+ [F_{\Psi_+}, G_{\Psi_+}] \rangle \\ & - 2\rho_e \langle \Psi_- [F_{\Psi_-}, G_{\Psi_-}] \rangle. \end{aligned} \quad (26)$$

The above sums of independent brackets of the three variables are known as a direct product.³⁵ Since the individual brackets satisfy the Jacobi identity, their sums in Eqs. (25) and (26) also do. By virtue of the coordinate invariance of the Jacobi identity, it follows that the parallel and perpendicular brackets given by Eqs. (13) and (14) also satisfy the Jacobi identity. Appendix B shows that the complete bracket given in Eq. (12) also satisfies this identity and is thus a proper Poisson bracket.

IV. DISPERSION RELATION

A. Exact

To make contact with previously known results, we introduce the resistive force in the electron momentum equation,

$$\frac{\partial}{\partial t} (\psi - d_e^2 J) - d_e^2 [\phi, J] + \nabla_{\parallel} (n - \phi) = \eta J.$$

Taking the \hat{z} axis to lie in the direction of the equilibrium magnetic field, the \hat{x} axis to lie in the direction of the equilibrium density gradient, and $\hat{y} = \hat{z} \times \hat{x}$, the linearized equations consist of

$$\omega n_i - \omega_{*e} \Phi = 0, \quad (27)$$

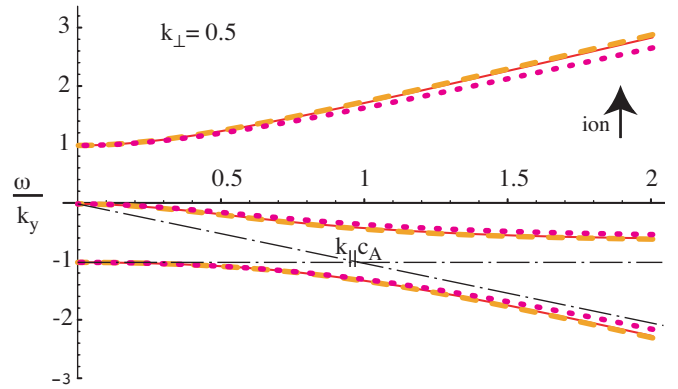


FIG. 1. (Color online) Graph of the dispersion relation for $\tau=1$, $d_e=0$, and $k_{\perp}=0.5$. The three groups of curves correspond to the two branches of the kinetic Alfvén wave and the drift wave. Within each group the solid line represents the kinetic result, the dashed line represents the Padé approximation, and the dotted line represents the FLR expansion. For this value of k_{\perp} the FLR result agrees within 10% for all branches. The dashed-dotted lines represent the dispersion relation in the limit $k_{\perp} \rightarrow \infty$ where the Alfvén and drift waves propagating in the electron direction decouple. The arrow indicates the ion drift direction.

$$\omega n_e - \omega_{*e} \phi - k_{\parallel} k_{\perp}^2 c_A^2 \psi = 0, \quad (28)$$

$$\omega(1 + k_{\perp}^2 d_e^2) \psi - \omega_{*e} \psi + k_{\parallel} (\phi - n_e) = -i \eta k_{\perp}^2 \psi, \quad (29)$$

and the linearized quasineutrality equation. Here $\omega_{*e} = -k_y n_0'(x) = -k_y$ in our normalized units. This system yields the dispersion relation

$$\begin{aligned} & \left(1 - \frac{\omega_{*i}}{\omega} \right) \frac{[\Gamma_0(b) - 1]}{\tau} \left[1 - \frac{\omega_{*e}}{\omega} + k_{\perp}^2 \left(d_e^2 + \frac{i\eta}{\omega} - \frac{k_{\parallel}^2 c_A^2}{\omega^2} \right) \right] \\ & = -k_{\perp}^2 \left(1 - \frac{\omega_{*e}}{\omega} \right) \frac{k_{\parallel}^2 c_A^2}{\omega^2}, \end{aligned} \quad (30)$$

where $b = \tau k_{\perp}^2$ and $\omega_{*i} = -\tau \omega_{*e} = \tau k_y$. Taking $d_e = 0$ in the above dispersion relation, we recover the result of Kadomtsev and Pogutse.³⁶

The dispersion relation is cubic in the frequency so that it is easily solved. We have graphed the angular frequency as a function of k_{\parallel} in Figs. 1 and 2. For large k_{\parallel} the roots with the smallest and largest frequencies correspond to the two branches of the kinetic Alfvén wave, while the intermediate root corresponds to the drift wave. If one follows the dispersion curves toward smaller k_{\parallel} , the drift wave and the lower branch of the kinetic Alfvén wave (traveling in the electron-drift direction) undergo mode conversion at $k_{\parallel} c_A \sim 1$. For $k_{\parallel} c_A \ll 1$, the root with the lowest frequency is the drift-Alfvén wave; its value of -1 at $k_{\parallel} = 0$ corresponds to $\omega = \omega_{*e}$ in un-normalized units. The upper root, which attains the value of $+1$ at $k_{\parallel} = 0$ (corresponding to the un-normalized value of ω_{*i}), is sometimes called the ion drift wave.

Note that whenever magnetic shear is present, k_{\parallel} will vary across the plasma. When this is the case, the set of values ω corresponding to a real value of k_{\parallel} represents the continuous spectrum for the inhomogeneous plasma. The band of frequencies lying between 0 and $\omega_{*i} = \tau k_y$ constitutes a gap in which there is no real root for k_{\parallel} . This gap can harbor discrete modes that do not suffer from continuum

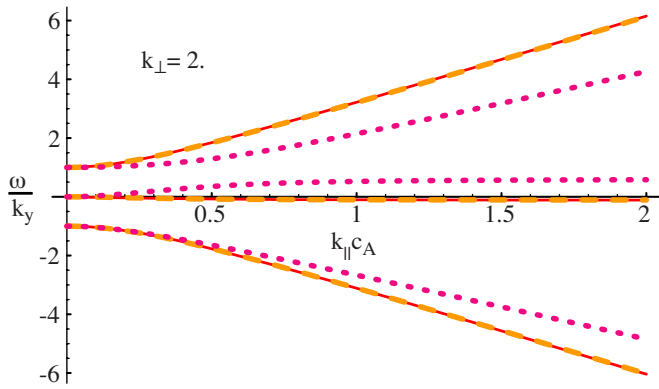


FIG. 2. (Color online) Graph of the dispersion relation for $\tau=1$, $d_e=0$, and $k_{\perp}=2.0$. The three groups of curves correspond to the two branches of the kinetic Alfvén wave and the drift wave as in Fig. 1. The curve for the Padé approximation is almost indistinguishable from the exact result. The frequency of the drift wave given by the FLR model (the central dotted curve), by contrast, has the wrong sign.

damping. The role of this gap in the dynamics of the sawtooth instability and of the neoclassical tearing mode is discussed in Refs. 37 and 38, respectively.

B. Padé approximant

The Padé version of our electromagnetic model is obtained by using $\Gamma_0^{1/2}(b)=(1+b/2)^{-1}$ and taking

$$n_e = (1 + b/2)^{-1} n_i - (1 - \Gamma_0) \phi / \tau. \tag{31}$$

With these approximations the dispersion relation becomes

$$(\omega - \omega_{*i})(\omega - \omega_{*e}) = [1 - \omega_{*e}/\omega + (1 + \tau)k_{\perp}^2]k_{\perp}^2 c_A^2. \tag{32}$$

The dispersion relation for the kinetic, Padé, and FLR models are compared in Figs. 1 and 2 where the Padé model is seen to give an excellent approximation whereas, unsurprisingly, the FLR model is inadequate for moderate to large values of k_{\perp} . In particular, the FLR dispersion relation fails to display the gap in the continuous spectrum between 0 and ω_{*i} . The gap is evident in Fig. 3 where the gyrofluid dispersion relation is graphed for a logarithmic scan of k_{\perp} . This

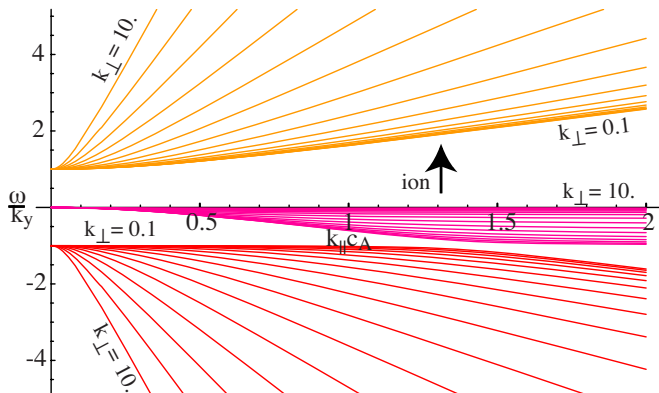


FIG. 3. (Color online) Graph of the gyrofluid dispersion relation showing the spectral gap between 0 and ω_{*i} for $\tau=1$ and for $\log_{10} k_{\perp}$ ranging from -1 to 1 in steps of 0.125.

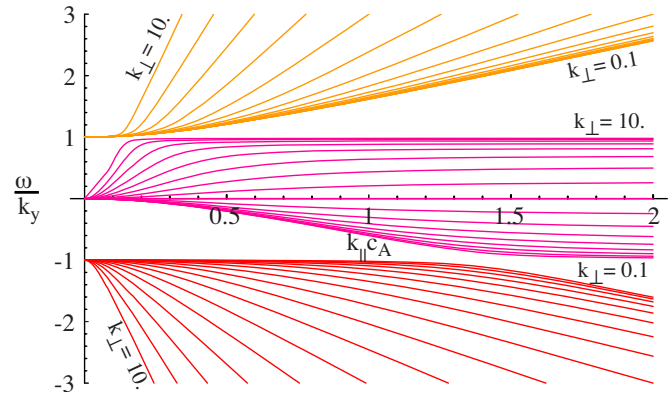


FIG. 4. (Color online) Graph of the FLR dispersion relation showing the absence of spectral gap between 0 and ω_{*i} for the same parameters as in Fig. 3.

figure is in contrast to Fig. 4 showing the absence of gap in the corresponding scan of the dispersion relation for the FLR model.

An example of the role of the dispersion relation in non-linear drift-Alfvén dynamics is provided by the evolution of magnetic islands in fusion devices.³⁹ When their phase velocity is between the ion and electron drift velocities, magnetic islands experience a braking force due to the radiation of drift-acoustic waves. Calculations of the magnitude of this force and of the effect of the radiation on the island amplitude using a FLR model have shown that the radiative effects are weak in the frequency band where the FLR model incorrectly predicts wave propagation across the magnetic field ($k_{\perp}^2 > 0$).⁴⁰ The reason for this is that the FLR model predicts a cutoff ($k_{\perp} \rightarrow 0$) at the electron drift frequency but a resonance ($k_{\perp} \rightarrow \infty$) at the ion drift frequency, so that the fictitious waves in the ion direction predicted by the FLR model are strongly damped by collisional transport processes. The importance of drift-wave radiation in the electron direction, however, is confirmed by direct numerical simulations.⁴¹

V. EQUILIBRIUM

A. General case

In this section we examine the calculation of two-dimensional equilibria with $\partial/\partial z=0$. We note that the results apply to ideal coherent structures since such structures represent states with localized properties that are fixed in time when viewed in a moving frame. That is, they are a particular kind of equilibrium solutions.

It is instructive to consider the task of calculating the equilibrium states by solving the equations of motion (1)–(3) directly after setting all of the time derivatives to zero:

$$\bar{\mathbf{v}}_E \cdot \nabla n_i = 0, \tag{33}$$

$$\mathbf{v}_E \cdot \nabla n_e = c_A^2 \nabla_{\parallel} J, \tag{34}$$

$$\nabla_{\parallel} (n_e - \phi) = d_e^2 \mathbf{v}_E \cdot \nabla J, \tag{35}$$

where $\mathbf{v}_E = \hat{\mathbf{z}} \times \nabla \phi$ is the electric drift velocity and $\bar{\mathbf{v}}_E = \bar{\mathbf{z}} \times \nabla \Phi$ is its gyroaverage. Equations (33)–(35) contain combinations of convective derivatives along different vector

fields, namely, the magnetic field and electric drift-velocity field. Unfortunately, there exists no systematic procedure for solving such a system of equations. In the absence of a Hamiltonian formulation, one must begin by checking whether the solubility conditions are satisfied. In the presence of convection cells, for example, the solubility of Eq. (34) requires that

$$\oint \frac{dl}{|\mathbf{v}_E|} \nabla_{\parallel} J = 0, \quad (36)$$

where the integral is calculated on a closed streamline. Furthermore, integrating Eq. (34) around the cross section of a flux tube requires that

$$\oint \frac{dl}{|\nabla\psi|} \mathbf{v}_E \cdot \nabla n_e = 0. \quad (37)$$

Equation (35) must also satisfy similar solubility conditions. Note that coherent structures, in particular, are typically characterized by closed streamlines as well as closed flux surfaces and thus have to satisfy both of the above solubility conditions. A violation of the solubility conditions indicates an inconsistency of the fluid closure under consideration. Such a violation can sometimes be detected by evaluating the solubility integrals near the center of a vortex tube or near a magnetic axis using a Taylor expansion of their arguments.²³

Clearly, the direct approach is impractical for all but the simplest models. Fortunately, Hamiltonian formulations enable the use of a powerful variational method. When a Hamiltonian formulation is available, the equilibrium equations may be expressed as $\{\xi_j, H\} = 0$ for all j . Invoking the invariance of Casimirs leads to the more general condition

$$\{\xi_j, F\} = 0, \quad (38)$$

where $F = H + C$. The solution of Eq. (38) is

$$\delta F / \delta \xi_j = 0 \quad (39)$$

for all j . That is, the equilibria are extremals of the functional F . It is easy to see that Eq. (39) provides first integrals of Eq. (38) or, equivalently, of Eqs. (33)–(35), since the Poisson brackets involve differential operators. Thus, the Hamiltonian approach directly yields first integrals of the equilibrium equations. It follows that all of the integrability conditions such as Eqs. (36) and (37) are automatically satisfied for a Hamiltonian system. Another advantage of the variational approach is that the second variation of F describes the linear stability of the system.³⁴ F itself may also be used to construct nonlinear stability criteria based on convexity arguments.³⁴

The variational approach is particularly useful when calculating the steady-state solution reached asymptotically after a time-dependent process. In particular, it allows the determination of the relationship between the profiles that appear in the equilibrium equations and the free functions (f, g_{\pm}) that appear in the Casimirs. One application is to the calculation of a bifurcated equilibrium solution corresponding to the saturated state of the system after an ideal instability.^{14,42} Another application is to the determination of

the final state after the collision of two coherent structures. The infinite family of conserved quantities that the Casimir represents contributes to the solitary nature of coherent structures by virtue of the fact that they constrain the equilibrium solution. That is, if two coherent structures separate after a collision, the conservation of the Casimirs implies that they will have the same initial and final states. Since they do not completely determine the state of the system, the Casimirs do not prevent the mixing of coherent structures during collisions.

For the system under consideration in this paper, demanding that F be extremal with respect to all the variables leads to

$$-J + g'_+(\Psi + \rho_e n_e) + g'_-(\Psi - \rho_e n_e) = 0, \quad (40)$$

$$n_e - \phi + \rho_e [g'_+(\Psi + \rho_e n_e) - g'_-(\Psi - \rho_e n_e)] = 0, \quad (41)$$

$$\Phi + f'(n_i) = 0. \quad (42)$$

The quasineutrality condition, Eq. (5), completes the above system of equations. Assuming that the function f' in Eq. (42) is invertible, this equation and the quasineutrality equation may be used to eliminate n_e and n_i in terms of ϕ and ψ , leaving a system of two nonlinear coupled integrodifferential equations for ϕ and ψ ,

$$\begin{aligned} & \Gamma_0^{1/2} f'^{-1}(\Gamma_0^{1/2} \phi) + (\Gamma_0 - 1) \phi / \tau - \phi \pm \rho_e J \\ & = \pm 2\rho_e g'_{\mp}[\Psi \mp \rho_e \Gamma_0^{1/2} f'^{-1}(\Gamma_0^{1/2} \phi) \mp \rho_e (\Gamma_0 - 1) \phi / \tau]. \end{aligned} \quad (43)$$

To obtain the equilibrium equations in a frame moving at speed c in the y direction, one can use the identities stated at the end of Sec. II to conclude that it is sufficient to replace ϕ in these equations by $\phi - cx$. Equivalent equations can be obtained by adding the momentum invariant to the variational principle.

Solving these equations is difficult but is fortunately unnecessary in general, since the smallness of the ratio of the electron and ion masses results in separation of scales. It is thus possible in general to solve simpler equations and match them asymptotically. In the following section we consider the solution of the equilibrium problem on scales large compared to the electron skin depth.

B. Limit of vanishing electron mass

For $k_{\perp} d_e \ll k_{\perp} \rho_s \sim 1$, the electron inertia may be neglected. In this regime the solutions of the equilibrium equations, obtained by neglecting the time derivatives in Eqs. (1)–(3), are

$$n_i = K(\Phi), \quad (44)$$

$$n_e = \phi + H(\psi), \quad (45)$$

$$\nabla^2 \psi = I(\psi) - \phi H'(\psi), \quad (46)$$

where $H'(\psi) = dH/d\psi$. Substituting the above results for n_i and n_e into the quasineutrality equation yields an equation for ϕ alone:

$$\Gamma_0^{1/2} K(\Gamma_0^{1/2} \phi) - \phi + (\Gamma_0 - 1) \phi / \tau = H(\psi). \quad (47)$$

We may simplify this equation by applying the operator $\Gamma_0^{1/2}$ on both sides:

$$\Gamma_0 [K(\Phi) + \Phi / \tau] - (1 + 1/\tau) \Phi = \Gamma_0^{1/2} H(\psi).$$

Inverting the Γ_0 operator, we obtain the following equation for Φ :

$$(1 + 1/\tau) \Gamma_0^{-1} \Phi - [K(\Phi) + \Phi / \tau] = -\Gamma_0^{-1/2} H(\psi).$$

Using the Padé approximant of Γ_0 , there follows

$$(1 + 1/\tau) \rho_i^2 \nabla^2 \Phi + [K(\Phi) - \Phi] = \Gamma_0^{-1/2} H(\psi). \quad (48)$$

This equation has a form similar to that of the Grad-Shafranov equation (46), and the two coupled equations can be solved by conventional methods. These coupled equations have a rich variety of stationary and traveling-wave solutions depending on the choice of the free functions.

VI. SUMMARY

We have investigated the equations obtained from the general electromagnetic gyrofluid model of Ref. 19 by keeping only the lowest-order moment (the continuity equation) for the ions and the lowest two parallel moments (the continuity equation and Ohm's law) for the electrons. We have shown that these equations are Hamiltonian and have presented the corresponding noncanonical Lie–Poisson brackets. The system possesses a Casimir functional given by Eq. (21) that depends on three arbitrary functions. The existence of a proper Poisson bracket describing the dynamics guarantees that the equilibrium equations obtained by neglecting the time derivatives (possibly in a frame of reference moving at constant velocity) may be integrated once to obtain Grad–Shafranov-like equations that determine the magnetic flux (i.e., the component of the vector-potential along the background field) and the electrostatic potential. The corresponding equilibrium equations are given by Eq. (43) for the general case and by Eqs. (46) and (48) in the case of negligible electron inertia. The functions entering into the Casimir functional determine the profiles of the various fields in the equilibrium state.

Possible applications of the electromagnetic gyrofluid model presented here include any electromagnetic problems where both diamagnetic drifts and nonlinear effects are important. In fusion devices, two examples are the sawtooth crash in the core^{9,37,43–45} and the peeling-ballooning modes in the edge.^{37,45–48}

ACKNOWLEDGMENTS

We wish to thank Dr. Pegoraro and Dr. Kuvshinov for responding to our questions concerning Ref. 28. This work was supported by the U.S. DOE under Contract Nos. DE-FG03-96ER-54346 and DE-FC02-04ER54785.

APPENDIX A: JACOBI IDENTITY FOR THE SPK MODEL

In this appendix we show that the SPK model²⁸ fails to satisfy the Jacobi identity, Eq. (15). We use the notation of Ref. 28 throughout. The functional derivatives of the brackets are

$$\frac{\delta}{\delta \xi_3} \{F, G\} = ad_e \beta_e^{-1/2} ([F_{\xi_3}, G_{\xi_3}] + \dots),$$

$$\frac{\delta}{\delta \xi_2} \{F, G\} = ad_e \beta_e^{-1/2} ([F_{\xi_2}, G_{\xi_2}] + [\mathbf{L}F_{\xi_3}; \mathbf{L}G_{\xi_3}] + \dots),$$

where the “...” indicate terms that do not contribute to the Jacobi identity, $[\mathbf{A}; \mathbf{B}] = \sum_j [A_j, B_j]$, and

$$\xi_2 = d_e \beta_e^{1/2} \left(\ln \frac{n}{n_0} \right), \quad \xi_3 = -d_e \beta_e^{1/2} \left(\ln \frac{n}{n_0} + \tau(1 - \Gamma_0) \phi \right)$$

as in Ref. 28. The nested bracket is thus

$$\begin{aligned} \{ \{F, G\}, H \} &= a^2 d_e^2 \beta_e^{-1} \langle \xi_3 [[F_{\xi_3}, G_{\xi_3}], H_{\xi_3}] \\ &\quad + \xi_2 [[F_{\xi_2}, G_{\xi_2}], H_{\xi_2}] + [[\mathbf{L}F_{\xi_3}; \mathbf{L}G_{\xi_3}], H_{\xi_2}] \\ &\quad + [\mathbf{L}[F_{\xi_3}, G_{\xi_3}]; \mathbf{L}H_{\xi_3}] \rangle. \end{aligned}$$

The first two terms cancel in the sum of cyclic permutations, but the last two do not. To show explicitly that the bracket does not obey the Jacobi identity, we use the following counterexample:

$$F = \langle x^2 \xi_3 \rangle, \quad G = \langle y^2 \xi_3 \rangle, \quad H = \langle \xi_3^2 \rangle.$$

All the functional derivatives of the above three functionals vanish except

$$F_{\xi_3} = x^2, \quad G_{\xi_3} = y^2, \quad H_{\xi_3} = 2\xi_3.$$

Keeping only the lowest-order term in \mathbf{L} , $\mathbf{L} \approx \rho_i \nabla$, we find

$$\begin{aligned} \mathcal{J} &= a^2 d_e^2 \beta_e^{-1} \rho_i \langle \xi_2 ([y, \partial_x \xi] + [x, \partial_y \xi] - [x \partial_{yy} \xi_3, y] \\ &\quad - [y \partial_{xx} \xi_3, x]) \rangle, \\ &= a^2 d_e^2 \beta_e^{-1} \rho_i \langle \xi_2 (y \partial_{xy} \xi_3 - x \partial_{yx} \xi_3) \rangle. \end{aligned}$$

where \mathcal{J} , defined in Eq. (15), is the sum of cyclic permutations of the nested brackets in the Jacobi identity. Clearly, \mathcal{J} does not vanish in general.

APPENDIX B: JACOBI IDENTITY USING NORMAL FIELDS

In this appendix we use the normal fields to show that the complete bracket, formed in Eq. (12) by combining the parallel and perpendicular brackets, satisfies the Jacobi identity. Because of the decoupling of variables in the direct product form, it is only necessary to prove the Jacobi identity for the following:

$$\begin{aligned} \{F, G\}^{(+)} &= \{F, G\}_{\parallel}^{(+)} + \{F, G\}_{\perp}^{(+)} \\ &= 2\rho_e \langle -G_{\Psi_+} \partial_z F_{\Psi_+} + \Psi_+[F_{\Psi_+}, G_{\Psi_+}] \rangle. \end{aligned} \quad (\text{B1})$$

The Ψ_- bracket is identical and there is no parallel contribution for the n_i bracket.

It is easy to see that the parallel and perpendicular brackets separately satisfy the Jacobi identity. We must show that their sum also does:

$$\begin{aligned} \{\{F, G\}^{(+)}, H\}^{(+)} + \text{cyc.} &= \{\{F, G\}_{\perp}^{(+)}, H\}_{\perp}^{(+)} + \{\{F, G\}_{\parallel}^{(+)}, H\}_{\parallel}^{(+)} \\ &\quad + \{\{F, G\}_{\parallel}^{(+)}, H\}_{\perp}^{(+)} \\ &\quad + \{\{F, G\}_{\perp}^{(+)}, H\}_{\parallel}^{(+)} + \text{cyc.}, \end{aligned} \quad (\text{B2})$$

The first and fourth terms in Eq. (B2) involve elementary brackets that are already known to satisfy the Jacobi identity. The third term vanishes because

$$\frac{\delta\{F, G\}_{\parallel}^{(+)}}{\delta\Psi_+} = 0 + \dots, \quad (\text{B3})$$

where the dots represent second-variation terms that do not contribute to the sum of cyclic permutations (see Ref. 33). There remains to show that

$$\{\{F, G\}_{\perp}^{(+)}, H\}_{\parallel}^{(+)} + \text{cyc.} \equiv 0. \quad (\text{B4})$$

Note that

$$\frac{\delta\{F, G\}_{\perp}^{(+)}}{\delta\Psi_+} = 2\rho_e [F_{\Psi_+}, G_{\Psi_+}] + \dots. \quad (\text{B5})$$

Inserting this into Eq. (B4) gives

$$\begin{aligned} \{\{F, G\}^{(+)}, H\}^{(+)} + \text{cyc.} &= -4\rho_e^2 \langle H_{\Psi_+} \partial_z [F_{\Psi_+}, G_{\Psi_+}] \\ &\quad + F_{\Psi_+} \partial_z [G_{\Psi_+}, H_{\Psi_+}] \\ &\quad + G_{\Psi_+} \partial_z [H_{\Psi_+}, F_{\Psi_+}] \rangle. \end{aligned} \quad (\text{B6})$$

Upon integrating the first term of Eq. (B6) by parts and making use of Gauss' identity in the form $\langle f[g, h] \rangle = -\langle g[f, h] \rangle$, we see that the first term cancels the sum of the second and third, thereby establishing the Jacobi identity for the complete bracket.

¹A. Hasegawa and K. Mima, *Phys. Rev. Lett.* **37**, 690 (1976).

²J. F. Drake, P. N. Guzdar, and A. B. Hassam, *Phys. Rev. Lett.* **61**, 2205 (1988).

³K. Hallatschek, *Phys. Rev. Lett.* **84**, 5145 (2000).

⁴K. Hallatschek, *Phys. Rev. Lett.* **93**, 065001 (2004).

⁵J. F. Drake, R. G. Kleva, and M. E. Mandt, *Phys. Rev. Lett.* **73**, 1251 (1994).

⁶A. Y. Aydemir, *Phys. Fluids B* **4**, 3469 (1992).

⁷R. G. Kleva, J. F. Drake, and F. L. Waelbroeck, *Phys. Plasmas* **2**, 23 (1995).

⁸P. A. Cassak, M. A. Shay, and J. F. Drake, *Phys. Rev. Lett.* **95**, 235002 (2005).

⁹D. Biskamp and T. Sato, *Phys. Plasmas* **4**, 1326 (1997).

¹⁰D. Grasso, F. Califano, F. Pegoraro, and F. Porcelli, *Phys. Rev. Lett.* **86**, 5051 (2001).

¹¹B. N. Rogers, W. Dorland, and M. Kotschenreuther, *Phys. Rev. Lett.* **85**, 5336 (2000).

¹²R. D. Hazeltine, M. Kotschenreuther, and P. J. Morrison, *Phys. Fluids* **28**, 2466 (1985).

¹³P. J. Morrison and R. D. Hazeltine, *Phys. Fluids* **27**, 886 (1984).

¹⁴E. Tassi, P. J. Morrison, F. L. Waelbroeck, and D. Grasso, *Plasma Phys. Controlled Fusion* **50**, 085014 (2008).

¹⁵C. T. Hsu, R. D. Hazeltine, and P. J. Morrison, *Phys. Fluids* **29**, 1480 (1986).

¹⁶A. Zeiler, J. F. Drake, and B. Rogers, *Phys. Plasmas* **4**, 2134 (1997).

¹⁷G. W. Hammett, W. Dorland, and F. Perkins, *Phys. Fluids B* **4**, 2052 (1992).

¹⁸W. Dorland and G. W. Hammett, *Phys. Fluids* **5**, 812 (1993).

¹⁹P. B. Snyder and G. W. Hammett, *Phys. Plasmas* **8**, 3199 (2001).

²⁰N. F. Loureiro and G. W. Hammett, *J. Comput. Phys.* **227**, 4518 (2008).

²¹S. Hamaguchi and W. Horton, *Phys. Fluids B* **2**, 1833 (1990).

²²J. A. Krommes and R. A. Kolesnikov, *Phys. Plasmas* **11**, L29 (2004).

²³F. L. Waelbroeck, P. J. Morrison, and W. Horton, *Plasma Phys. Controlled Fusion* **46**, 1331 (2004).

²⁴C. B. Kim, W. Horton, and S. Hamaguchi, *Phys. Fluids B* **5**, 1516 (1993).

²⁵D. J. Wu, D. Y. Wang, and G. L. Huang, *Phys. Plasmas* **4**, 611 (1997).

²⁶J. L. Terry, S. J. Zweben, K. Hallatschek, B. LaBombard, R. J. Maqueda, B. Bai, C. J. Boswell, M. Greenwald, D. K. W. M. Nevins, C. S. Pitcher, B. N. Rogers, D. P. Stotler, and X. Q. Xu, *Phys. Plasmas* **10**, 1739 (2003).

²⁷R. D. Hazeltine, C. T. Hsu, and P. J. Morrison, *Phys. Fluids* **30**, 3204 (1987).

²⁸T. J. Schep, F. Pegoraro, and B. N. Kuvshinov, *Phys. Plasmas* **1**, 2843 (1994).

²⁹B. N. Kuvshinov, F. Pegoraro, and T. J. Schep, *Phys. Lett. A* **191**, 296 (1994).

³⁰D. Strintzi, B. D. Scott, and A. J. Brizard, *Phys. Plasmas* **12**, 052517 (2005).

³¹D. Grasso, F. Califano, F. Pegoraro, and F. Porcelli, *Plasma Phys. Rep.* **26**, 512 (2000).

³²S. Vincena, W. Gekelman, and J. Maggs, *Phys. Rev. Lett.* **93**, 105003 (2004).

³³P. J. Morrison, *AIP Conf. Proc.* **88**, 13 (1982).

³⁴P. J. Morrison, *Rev. Mod. Phys.* **70**, 467 (1998).

³⁵J. L. Thiffeault and P. J. Morrison, *Physica D* **136**, 205 (2000).

³⁶B. B. Kadomtsev and O. P. Pogutse, in *Reviews of Plasma Physics*, edited by M. A. Leontovich (Consultants Bureau, New York, 1970), Vol. 5, pp. 249–400.

³⁷G. T. A. Huysmans, S. E. Sharapov, A. B. Mikhailovskii, and W. Kerner, *Phys. Plasmas* **8**, 4292 (2001).

³⁸F. L. Waelbroeck, J. Connor, and H. R. Wilson, *Phys. Rev. Lett.* **87**, 215003 (2001).

³⁹R. Fitzpatrick, P. Watson, and F. L. Waelbroeck, *Phys. Plasmas* **12**, 082510 (2005).

⁴⁰R. Fitzpatrick and F. Waelbroeck, *Phys. Plasmas* **12**, 122511 (2005).

⁴¹R. Fitzpatrick, F. L. Waelbroeck, and F. Militello, *Phys. Plasmas* **13**, 122507 (2006).

⁴²F. L. Waelbroeck, *Phys. Fluids B* **1**, 499 (1989).

⁴³D. Biskamp, *Phys. Rev. Lett.* **46**, 1522 (1981).

⁴⁴B. Rogers and L. Zakharov, *Phys. Plasmas* **2**, 3420 (1995).

⁴⁵I. Chapman, S. E. Sharapov, G. T. A. Huysmans, and A. B. Mikhailovskii, *Phys. Plasmas* **13**, 062511 (2006).

⁴⁶H. R. Wilson and R. L. Miller, *Phys. Plasmas* **6**, 873 (1999).

⁴⁷P. B. Snyder, H. R. Wilson, J. R. Ferron, L. L. Lao, A. W. Leonard, T. H. Osborne, and A. D. Turnbull, *Phys. Plasmas* **9**, 2037 (2002).

⁴⁸B. N. Rogers, J. F. Drake, and A. Zeiler, *Phys. Rev. Lett.* **81**, 4396 (1998).